Grain and Subgrain Structures Developed by Hot Working in As-Cast 434 Stainless Steel

E. Evangelista[1], P. Mengucci[1], J. Bowles[2] and H.J. McQueen[2]

[1] *Dept. of Mechanics, University of Ancona*
Ancona, 160131 Italy
[2] *Dept. of Mechanical Engineering, Concordia University*
Montreal, Quebec H3G 1M8, Canada

CONTENTS

ABSTRACT

Torsional deformation was conducted over a range of 800 to 1200 °C and 0.1 - 5 s^{-1} in order to establish the sinh-Arrhenius constitutive relationship. The continuously cast A1S1 400 alloys contained various quantities of segregated γ phase which was larger in volume fraction as the ferritizing additions decreased or as the austenitizing elements increased. The austenite appeared as discrete particles at the grain boundaries in 434 but as continuous layers and side plates in other alloys. The γ particles raised the strength and diminished the substructure recovery compared to that expected from the solute levels. The ferrite subgrains were larger as the strain rate declined and the temperature rose partly due to increased homogenization. The substructure was denser near the austenite particles and some statically recrystallized nuclei were observed.

INTRODUCTION

In an industrially related project, five grades of ferritic stainless with the macrostructure produced in continuously cast slabs were subjected to torsion testing. These steels are nominally ferritic and their strength was expected to vary with the amount of solute. However, in the cast condition, they had various amounts of austenite which greatly increased their strength since γ phase is not only stronger but also creates slip incompatibility (due to this, softer α particles raised the strength in as-cast austenitic steels /1-11/.

The 434 alloy (16.6Cr - 1.0Mo - 0.21Ni) exhibited small γ plates along the grain boundaries (GB) and a low density of larger Widmanstatten plates in the grains (Fig. 1). This alloy is usually preheated to 1150 °C for industrial rolling. The 430 steel (16.5Cr - 0.03Mo - 0.29Ni) exhibited somewhat greater density of γ phase nevertheless was rolled from 1100 °C. The 408 alloy (11.45Cr - 0.05Mo - 0.68Ni) had a high density of Widmanstatten γ (almost 50%) as a result of high Ni content and reduced ferrite-stabilizing Cr. It was rolled from 1200 °C to improve its ductility as well as lower its strength. The 40901 and 40900 alloys with 11.3/11.0Cr - 0.02/0.01Mo - 0.37/0.16Ni had levels of γ phase somewhat similar to 430 and 434, respectively; however, due to the softer matrix, they were preheated to 980 °C. The strengths observed in torsion for these as-cast materials were higher than those of homogenized alloys and rose roughly in the order of mounting rolling temperatures which differed from the order of rising total solutes. Only the strength of 434 will be discussed in detail and compared with published data /12-14/.

The ferritic steels are generally noted for their high level of dynamic recovery (DRV) /12-24/ which results in polygonized subgrains which are larger and more perfect with rising temperature T and declining strain rate $\dot{\varepsilon}$ or stress σ /25-26/. Due to the high level of DRV, such steels are not expected to undergo dynamic recrystallization (DRX) /15,16,22,26,27/ which is commonly observed in austenitic stainless steels /1-10/. However, it is possible that the hardening γ particles could produce DRX or static recrystallization SRX as a result of local regions of high dislocation density which enhance nuclei formation /2-5/. The microstructures of all the steels given a preliminary examination appear to follow the same general pattern. The microstructure of 434, as observed by optical,transmission electron (TEM) and scanning electron microscopy (SEM, channelling mode), will be presented in order to elucidate dynamic restoration mechanisms.

EXPERIMENTS

The experimental material was supplied by Atlas Steels of Tracy, Quebec, in the form of a block from one edge of a 200 mm thick continuously cast slab. Specimens were removed with their axes parallel to the casting direction and had a gage length, L, of 25 mm and diameter 2r = 6.3 mm. Protected by argon, the specimens were heated in a four element radiant furnace to 1200 °C for 10 min and cooled to the deformation temperature (controlled by a thermo-couple pressed against the gage section) and equilibrated for 5 min before deformation. The straining was performed in a computer-directed, servo-controlled hydraulically-powered torsion machine with digital data gathering as described previously /2,3,5,6,9/. The equivalent stress and strain were calculated by the following traditional formulae /3,5,6,9/:

$$\sigma = (\sqrt{3} / 2\pi r^3)\,(3 + n' + m)\,(\text{torque}) \qquad (1)$$

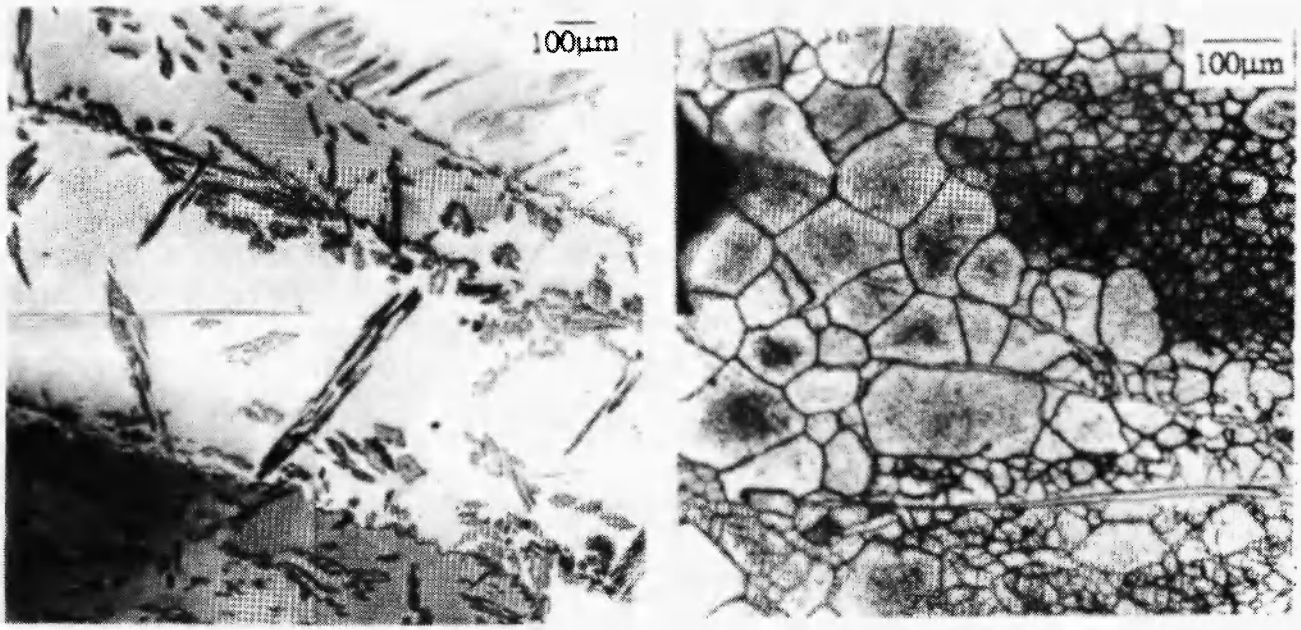

Fig. 1: As-cast microstructure (a) in a 434 alloy exhibiting ferritic grains with austenite particles along the grain boundaries and as plates within the grains (x50), and (b) a longitudinal section exhibiting δ stringers and both fine and coarse crystallites resulting from straining at 1100 °C, 1 s^{-1}, (x100).

$$\varepsilon = (2\pi r / L\sqrt{3})\,(\text{no. of twists}) \qquad (2)$$

where the gradient of ε and $\dot{\varepsilon}$ are corrected by means of n', the strain hardening coefficient (=0 for the plateau), and m, the strain rate sensitivity evaluated at each T from plots of log torque versus log $\dot{\varepsilon}$.

The optical and scanning microscopy specimens were ground and polished mechanically in the usual manner. The former were mounted so that transverse, longitudinal (diametral) and tangential sections could be examined. They were etched in a solution of 10 ml HNO_3, 10 ml $HC_2H_3O_2$, 15 ml HCl and 2-5 drops glycerol. The tangential sections for SEM were electrolytically polished in a solution of 20% perchloric acid in butoxyethanol at -4 °C and 18V. They were examined in the channelling mode to provide a back scattered electron image. The slices for thin foils were cut by a diamond saw perpendicular to the radius and about 0.5 mm from the surface. They were disced, and jet-thinned with the solution above.

STRENGTH AND CONSTITUTIVE RESULTS

Representative flow curves for as-cast 434 steel are presented in Fig. 2. The curves exhibit strain hardening to an approximate plateau in which there is a gradual decline. This is greater at higher stresses and so is partially linked to deformation heating. There is also some break up and solution of the non-equilibrium γ particles, to be described later; such a decrease is consistent with strength augmentation over homogenized materials as will be seen below. The tests were arrested at ε = 3.0 for metallographic examination; however, at 900 °C, the ductility lies between 3.5 and 1.8 and decreases as $\dot{\varepsilon}$ decreases.

In Fig. 3, the plots of log $\dot{\varepsilon}$ versus log sinh ασ and log sinh ασ against (1/T) show that the data conform to the equation /2,3,5,6,8-11/:

$$A\,(\sinh \alpha\sigma)^n = \dot{\varepsilon}\exp(Q_{HW}/RT) = Z \qquad (3)$$

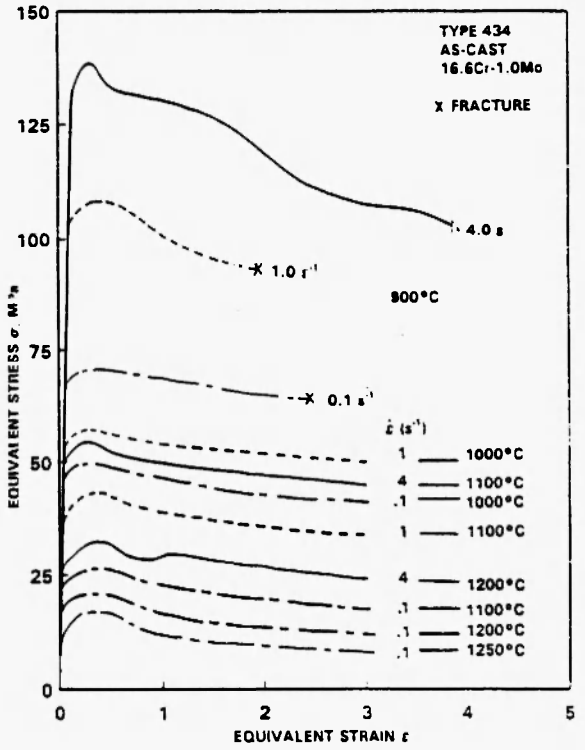

Fig. 2: Representative flow curves from hot torsion tests on 434 steel.

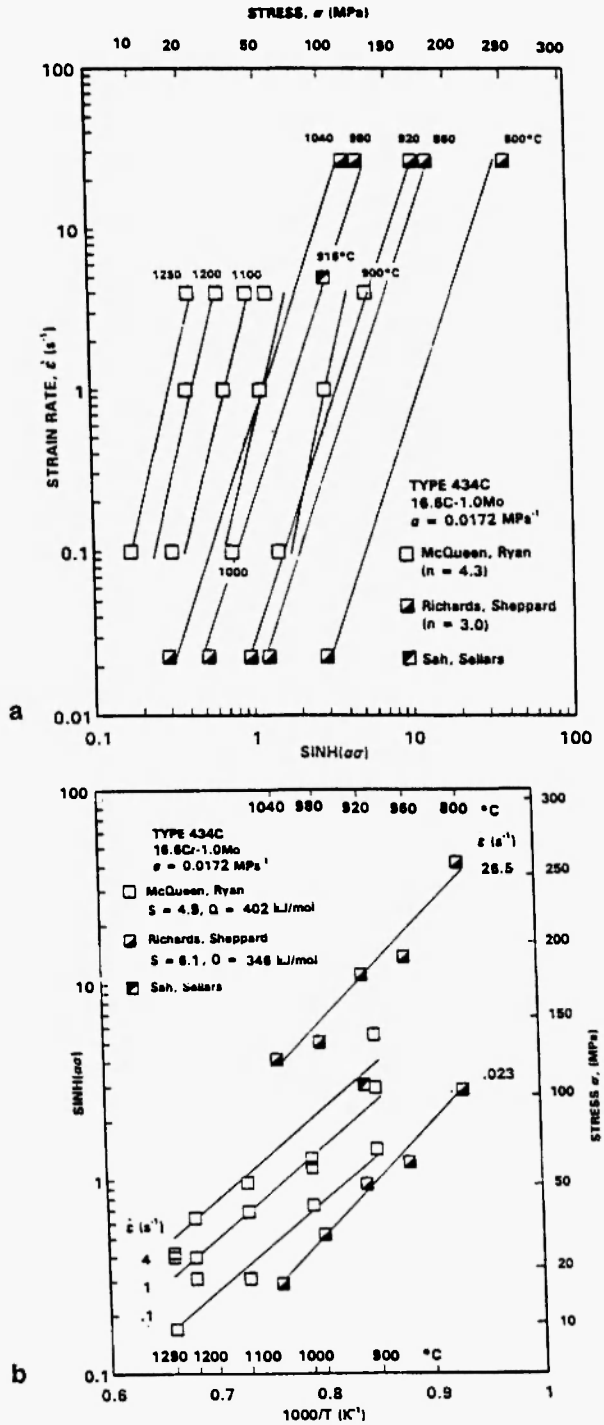

Fig. 3: The constitutive behavior of 434 alloy according to Eq. 3 is confirmed by the linear fits in (a) log $\dot{\varepsilon}$ versus log(sinh $\alpha\sigma$) and (b) log(sinh $\alpha\sigma$) versus (1/T). The results of Richards and Sheppard for steel 18-2 are included for comparison /13/.

where A, n', α (0.0172MPa^{-1} /13/), R (= 8.31 J/mol K) and Q_{HW} are constants. The Zener-Hollomon parameter, Z, is a T-compensated $\dot{\varepsilon}$ which remains constant during hot working tests. In the graphical analysis, the lines were constrained to be parallel, furnishing the value of n = 4.3 and of Q_{HW} = 402 kJ/mol. The data of Richards and Sheppard /13/ for worked-homogenized 18-2 alloy (18.0Cr-2.0Mo) is included. The σ values show a much greater $\dot{\varepsilon}$ dependence, n = 3. This combination of lower n and similar change of σ with T results in Q_{HW} = 345 kJ/mol. Even though there is additional 1% Mo and 1.4% Cr in 18-2, the flow stresses are similar to or lower than the present ones. These differences arise principally from the presence of the γ phase. This has not yet been confirmed by testing the homogenized steels but may be inferred from the effect of solidification segregated δ phase in strengthening as-cast γ stainless steels /1-5/.

MICROSTRUCTURAL RESULTS

The microstructures of 434 at all T exhibited elongated grains do not change within which subgrains are visible (see Fig. 4). The other marked feature is the stringers of γ phase which, at 1100 °C, seem to break up and decrease in volume fraction. Within the grains, the size of the subgrains increases as T rises. At 900 °C, the subgrains appear distorted with shadings that change from grain to grain. However, they are equiaxed and fairly uniform in size. At 1000 °C, the subgrains have divided into a bi-modal distribution lying in elongated bands; both groups, but more so the large ones, have appearances similar to grains. Evidence of the original GB has faded away (see earlier research /15,19-22/), except for the interfaces between the two size groupings or the γ stringers (Fig. 4c). The small subgrains are similar in size to those at 900 °C. In some cases, they are associated with the γ stringers but, in other cases, stand alone; of course, there could be γ phase below the surface. On the other hand, the large subgrains often butt directly on γ stringers. One might be led to think that the larger cells were recrystallized grains, but some evidence countering this follows. Similar microstructures were observed in 430, 409 and 408 steels.

The microstructure observed in SEM /28,29/ appears to consist of subgrains which give evidence of lattice curvatures within (see Fig. 5). Micrographs for other conditions confirm that there is a gradual increase in size with an increase in subgrain perfection as Z falls. The γ stringers appear to demarcate regions with different cell sizes. The γ phase appears to exhibit a cellular structure much finer than the α phase. There was evidence of the occasional formation of SRX grains (Fig. 5b) that were considerably larger than any of the cells and devoid of distortion.

The TEM examination revealed mainly subgrains at all deformation temperatures (Fig. 6); some regions were made up entirely of large subgrains and others of small ones. In both cases, the misorientations were low; although a statistical analysis was not carried out. When properly tilted, the subgrain boundaries (SGB) exhibited regular arrays of dislocations. In association with austenite stringers, both large and fine subgrains were observed in the ferrite with no evidence of augmented dislocation density. The α SGB appeared to run into the α-γ interfaces without any distortion. The austenite particles had undergone considerable elongation and had serrated boundaries. They contained elongated cells much smaller than those in the matrix; their characteristics were not examined thoroughly. Moreover, there was no outstanding evidence of DRX. Finally, there was no evidence of the development of regions containing several subgrains and having much higher misorientations as reported by Lombry et al. /20/.

DISCUSSION

The increased strength of the as-cast 434 (as well as of the 430) compared to published values for homogenized material /13/ appears to be the result of the stronger second phase which undergoes considerable elongation with the development of a poorly recovered substructure. The effects of the γ are greater at low temperatures when it is relatively harder. At higher temperatures, the γ has not only softened relative to the α matrix but has also diminished in volume thus providing much reduced reinforcement. The as-cast material exhibits a higher Q_{HW} than does the homogenized because of the greater change in strength due to the microstructural modifications. The present alloy is as strong at 1000 °C as Fe-25Cr /19,30/ and Fe-26Cr-Mo /24/ despite their higher solute content; these alloys also have a lower activation energy of about 331 kJ/mol. The high n and Q_{HW} values of the present alloy arise from the influence of the second phase on the strain hardening mechanism. This behavior is closely parallel to the differences between as-cast and homogenized austenitic stainless alloys /2-6,9/.

For the sake of discussion, one may take the simple position that the larger cellular structure found in some regions at high T arises from recrystallization. If produced through DRX, one would expect to find substructure developing within them, which is somewhat similar to that of fine cells. This is not the case, although there do appear to be greater dislocation densities than one might expect from SRX. Moreover, if the level of recovery is so high as to inhibit DRX, then it is not likely to cause SRX on such a large scale during rapid cooling. Finally, the evidence indicates that only a small propor-

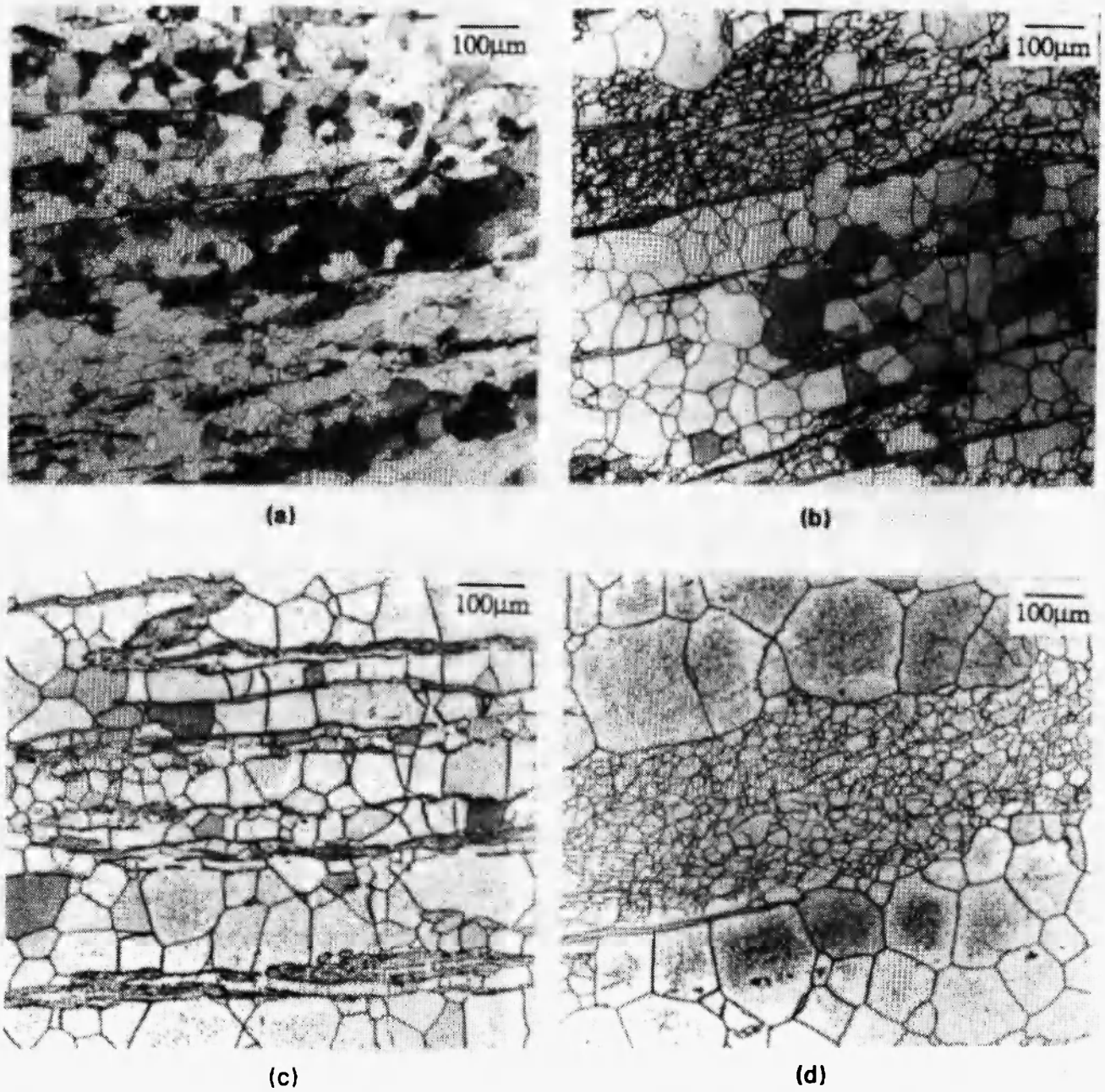

Fig. 4: Tangential sections of A1S1 434 torsion specimens observed by optical microscopy illustrate elongated grains containing subgrains and stringers of γ phase: a) 900°C, 4 s^{-1}; b) 1000°C, 4 s^{-1}; c) 1000°C,1 s^{-1}; and d) 1100°C, 1 s^{-1}. Magnification x100.

tion of the cell boundaries have high misorientation. The softening in the flow curve is possibly an indication of DRX; however, it is also likely to arise from deformation heating as well as from dissolution and spheroidization of the γ phase.

Consideration of the optical cellular structure resulting from DRV is consistent with the high level of recovery reported previously in homogenized ferritic Fe-Cr alloys /12-14/. Moreover, there is considerable evidence that in ferritic steels the sub-boundaries etch up more

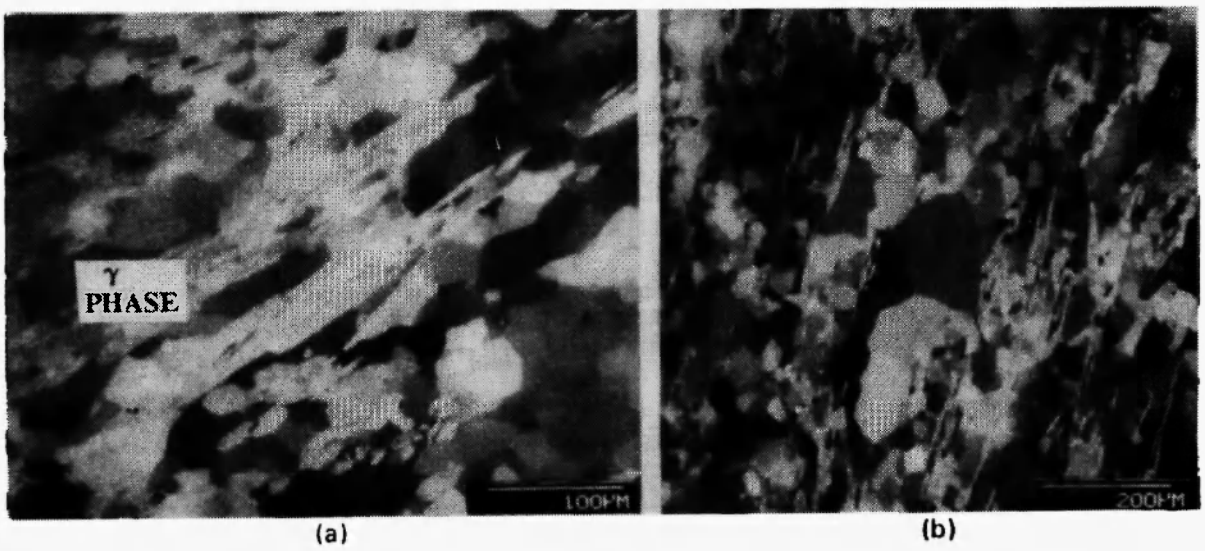

Fig. 5: Tangential section of 434 steel observed by SEM in channelling contrast to illustrate subgrain misorientations within the grains and the austenite phase: a) 1000°C, 0.1 s^{-1}; and b) 1100°C, 1 s^{-1}, exhibiting a cluster of statically recrystallized grains.

strongly as deformation proceeds /19-22/. Since the original boundaries become strongly serrated, they tend to become indistinguishable from the subgrains. Research in Al alloys has also shown that as the grains reach a thickness of about two subgrain diameters, they begin to pinch off where opposing serrations meet. This makes it increasingly difficult to distinguish GB /23,31/. In SEM, the large cells appear similar in character to the small cells which one interprets as subgrains due to their similarity to the low temperature specimens where the subgrains are clearly within elongated grains. In TEM, the large subgrain regions simply appear more recovered than small subgrain regions as one commonly observes in specimens of other metals deformed at high and low T. The level of recovery in the large cell region is comparable to that in Fe-18Cr-2Mo /12-14/, Fe-25Cr /19,20/ and Fe-26Cr-1Mo /24/, which partly accounts for the lower strength and Q_{HW} of the last two.

The difficulty with the bimodal subgrain structure is finding a suitable explanation for it. The simplest concept is that the fine cells are related to additional distortion created by either reduced or incompatible flow in the γ phase /32/. The regions of fine cells appearing isolated from the stringers could be associated with some above or below the plane of polishing. However, the presence of large cells touching the austenite and the absence of any distortion in the α immediately neighboring the γ grains contradict this. One could hypothesize that there are differences in solute level in different α grains as a result of solidification segregation; however, this has not been confirmed by microanalysis. One could also imagine that there are small precipitates present throughout at low T but dissolving in more and more grains as T increases, thus accounting for the sharp differences in size. Fine subgrains could form in shear bands but the geometry of the regions relative to the specimen macrostructure do not agree with this interpretation. Finally, one might be able to associate it with neighboring grains developing different orientations and, hence, strong differences in the shear stresses causing dislocation motion.

CONCLUSIONS

The as-cast 434 alloy has 20-30% higher net flow stress than homogenized material as a result of γ phase which deforms into stringers. The activation energy for as-cast is high because the effectiveness of the γ phase diminishes at high temperature partly because it dissol-

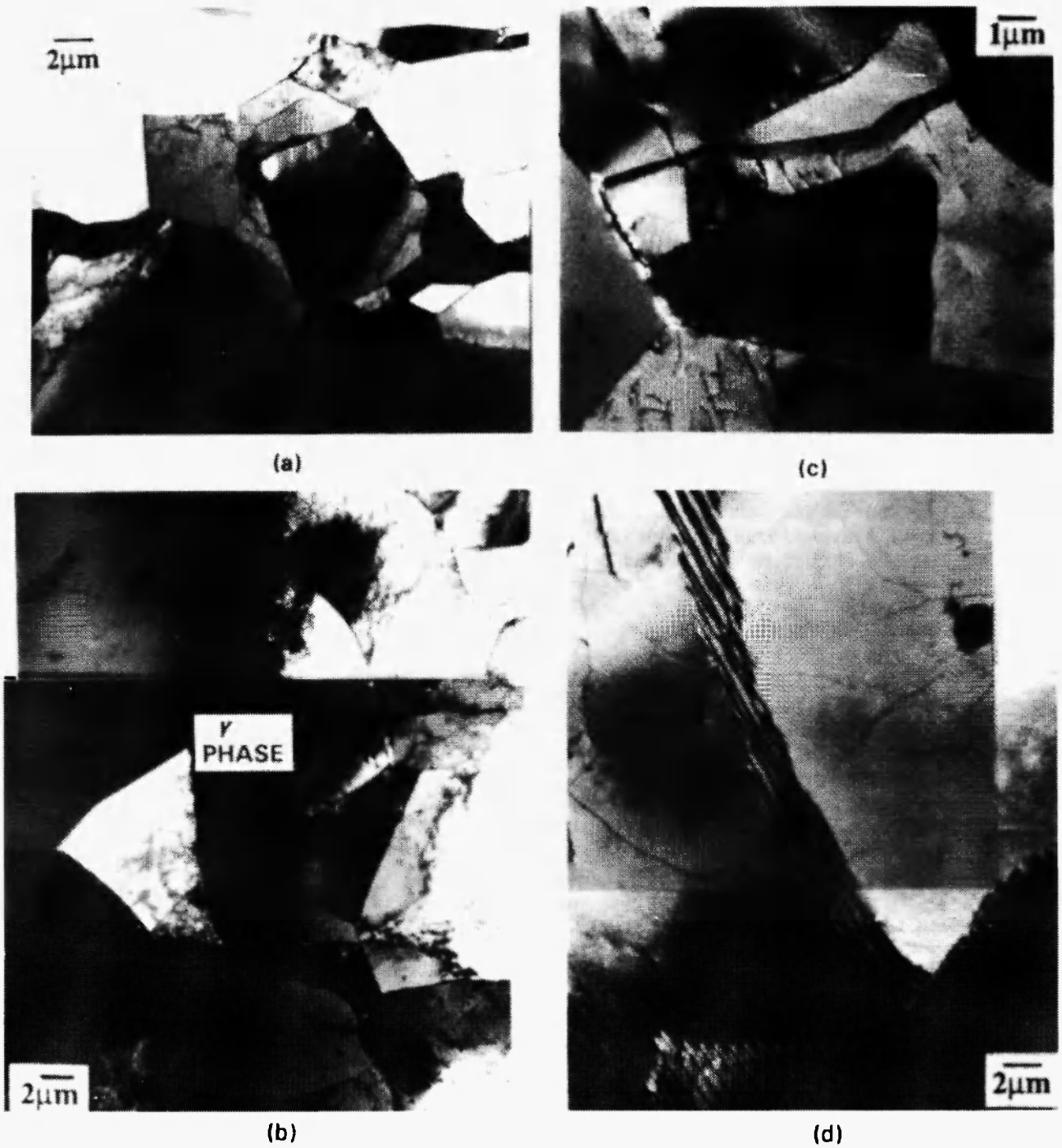

Fig. 6: TEM observations of slices cut normal to the radius of 434 torsion specimens: (a) 900°C, 1 s^{-1}; and (b,c,d) 1100°C, 1 s^{-1}.

ves. The substructure becomes more dynamically recovered as temperature rises; however, the specimen divides into regions of small subgrains and large subgrains. While γ phase constraints may be partially responsible, solute segregation or alternating textural elements may also contribute.

ACKNOWLEDGEMENTS

The authors acknowledge the financial support of the Natural Sciences and Engineering Research Council of Canada and the National Research Council (CNR) of Italy. They thank C. Smith for the torsion tests, T. Athanasoulias for the diagrams and S. Altimas for editing the text.

REFERENCES

1. Ryan, N.D., McQueen H.J. and Jonas, J.J., *Can. Metal. Q.*, **22**, 369-378 (1983).
2. Ryan, N.D. and McQueen, H.J., New Developments in Stainless Steel Technology, R.A. Lula (Ed.), ASM International, Materials Park, OH, 293-304 (1985).
3. Ryan, N.D. and McQueen, H.J., Intl. Symposium on Plasticity and Resistance to Metal Deformation, S. Bleeic (Ed.), Ferrous Metall. Inst., Niksic, Yugoslavia, 11-26 (1986).
4. McQueen, H.J., Ryan, N.D. and Evangelista, E., *Mat. Sci. Eng.*, **81**, 259-272 (1986).
5. Evangelista, E., Ryan, N.D. and McQueen, H.J., *Met. Sci. Tech.*, **5**, 50-58 (1987).
6. Ryan, N.D. and McQueen, H.J., *High Temp. Tech.*, **8**, 27-44 (1990).
7. Ryan, N.D. and McQueen, H.J., *High Temp. Tech.*, **8**, 185-200 (1990).
8. McQueen, H.J. and Ryan, N.D., Strength of Metals and Alloys, ICSMA 8, P.O. Kettunen et al. (Eds.), Pergamon Press, Oxford, 1323-1330 (1988).
9. Ryan, N.D. and McQueen, H.J., *J. Mat. Proc. Tech.*, **21**, 177-199 (1990).
10. McQueen, H.J., Evangelista, E. and Ryan, N.D., *La Metallurgia Italiana*, **81**, 119-131 (1989).
11. Ryan, N.D. and McQueen, H.J., Stainless Steels '87, Inst. of Metals, London, 498-507 (1987).
12. Sheppard, T. and Richards, P., *J. Mat. Sci.*, **22**, 1642-1650 (1987).
13. Richards, P. and Sheppard, T., *Mat. Sci. Tech.*, **2**, 841-846 (1986).
14. Richards, P. and Sheppard, T., *Mat. Sci. Tech.*, **2**, 836-840 (1986).
15. Bourell, D.L. and McQueen, H.J., *J. Mat. Shaping Tech.*, **5**, 53-73 (1987).
16. Glover, G. and Sellars, C.M., *Met. Trans.*, **4A**, 765-775 (1973).
17. Redfern, G.A. and Sellars, C.M., Deformation Under Hot Working Conditions, Iron Steel Inst., London, 29-37 (1986).
18. Redfern, G.A. and Sellars, C.M., *J. I.S.I.*, **208**, 576-582 (1970).
19. Rossard, C., *Metaux Corrosion Industries*, **35**, 190-205 (1960).
20. Lombry, R., Rossard, C. and Thomas, B.J., *Rev. Metall. CIT*, **78**, 975-988 (1981).
21. Barrett, C.R., Nix, W.D. and Sherby, O.D., *ASM Trans. Q.*, **59**, 311-378 (1966).
22. McQueen, H.J., Materials Technology: An Inter-American Approach, ASME, New York, 379-388 (1968).
23. McQueen, H.J. and Kassner, M.E., Superplasticity in Aerospace, H.C. Heikkenen and T.R. McNelley (Eds.), Met. Soc. AIME, Warrendale, PA, 77-96 (1988).
24. Schmidt, C.G., Young, C.M., Walser, B., Klundt, R.H. and Sherby, O.D., *Metal. Trans.*, **13A**, 447-456 (1982).
25. McQueen, H.J., Hot Working of Aluminum Alloys, T.G. Langdon (Ed.), TMS-AIME, Warrendale, PA, 31-54 (1991).
26. McQueen, H.J. and Jonas, J.J., *J. Appl. Metal Work*, **3**, 233-241, 410-420 (1985).
27. McQueen, H.J., Evangelista, E. and McQueen, H.J., Recrystallization 90, T. Chandra (Ed.), TMS AIME, Warrendale, PA, 89-100 (1990).
28. McQueen, H.J. and Hutchinson, W.B., Deformation of Polycrystals, N. Hansen et al. (Eds.), Riso Natl. Lab., Roskilde, Denmark, 335-342 (1981).

29. McQueen, H.J., Strength of Metals and Alloys (ICSMA 6), R.C. Gifkins (Ed.), Pergamon Press, Oxford, 517-522 (1982).

30. Sellars, C.M. and McG Tegart, W.J., *Mem. Sci. Rev. Metal.*, **63**, 731-746 (1966).

31. Solberg, J.K., McQueen, H.J., Ryum, N. and Nes, E., *Phil. Mag.*, **60**, 447-471 (1989).

32. Takeshita, T., Harase, J. and Yada, H., *Trans. ISIJ*, **27**, 432-438 (1987).